Effects of Slip Velocity and Hall Currents on Peristaltic Transport of Bingham-Papanastasiou Fluid with Heat Transfer

Nabil. T. M. Eldabe[a], Hameda M. Shawky[b], Amira S. Awaad[b,*]

[a] *Mathematics Department, Faculty of Education, Ain-Shams University, Cairo, Egypt*,

[b] *Mathematics Department, Faculty of Science (Girls), Al-Azhar University, Cairo, Egypt*.

Abstract

In this work, we investigated the effects of slip boundary condition and Hall currents on peristaltic motion of a non-Newtonian fluid which is obeying Bingham-Papanastasiou model, with heat transfer taking into account the thermal radiation and heat generation, through an asymmetric channel. This phenomena is modeled mathematically by a system of governing equations which are continuity, momentum and heat equations. These equations are solved analytically under low Reynolds number condition and long wavelength approximation. The stream function and temperature distribution are obtained as functions of physical parameters of the problem. The effects of the parameters on these solutions are discussed numerically and illustrated graphically through a set of figures. It is found that the physical parameters played important roles to control the velocity and temperature distribution.

Keywords: *Slip boundary condition; Hall currents; Peristaltic transport; Bingham-Papanastasiou fluid model; Thermal radiation; Heat generation.*

1 Introduction

The word peristalsis stems from the Greek word peristalikos. Peristalsis is defined as a wave of relaxation contraction (expansion) imparted by the walls of a flexible conduit, there by pumping the enclosed material, it is a nature's way of moving the content within hollow muscular structures by successive contraction of their muscular fibers [11, 12, 18, 19]. Peristalsis is now well-known to the physiologists to be one of the major mechanisms for fluid transport in many biological systems, it results physiologically from neuron muscular properties of the tubular smooth muscles [9, 23].

The peristaltic transport may be involved in many biological organs, e.g., swelling food through the esophagus, movement of chime in the gastrointestinal tract, urine transport from the kidney to the bladder through the ureter, transport of spermatozoa in the ducts efferent of male reproduction tract and in the cervical canal of the female, movement of ova in the fallopian tub, vasomotion of small blood vessels such as venules and capillaries as well as blood flow in

arteries, and in many other glandular ducts [9, 10, 18, 19, 23]. There are also many industrial applications of the peristaltic transport like, blood pumps in heart lung machine, transport of corrosive fluid, where the contact of the fluid with the machinery parts is prohibited [19].

Although the majority of fluids in the biosphere present Newtonian behavior, non-Newtonian behavior is observed in most industrial synthetic and non-synthetic fluids and in biological fluids, such as human blood and saliva. To quote a few examples, crude oil and drilling muds from the oil industry, paints, cosmetics, glues, soaps, detergents and many food products. Among them, an important class of non-Newtonian materials presents a yield stress limit which must be exceeded before significant deformation can occur the so-called Viscoplastic materials. In order to model the stress-strain relation in these fluids, some fitting have been proposed such as the linear Bingham equation and the non-linear Herschel-Bulkley and Casson models [22, 24, 17].

On the other hand Viscoplastic fluids are characterized by the absence of deformations when the applied load is below a fixed threshold. Bingham fluids area special class of Viscoplatic fluids named so after Bingham [5], who described several types of paint using this definition. Viscoplastic fluids constitute a very important class of non-Newtonian fluids. The modelling of Bingham materials is of crucial importance in industrial applications, since a large variety of materials (e.g. foams, pastes, slurries, oils, ceramics, etc.) exhibit the fundamental character of viscoplasticity, that is the capability off lowing only if the stress is above some critical value [13, 25, 6].

However, the Bingham model is not amenable to numerical analysis because in some complex applications, parts of material flow while the rest behaves as a solid. This causes difficulties in tracking the shape and the location of the yield surfaces and applying two different constitutive equations across them. In addition, at vanishing shear rates, the apparent viscosity in Bingham model becomes infinite, which leads to a discontinuity and numerical difficulties. To overcome these issues, Papanastasiou proposed a modified Bingham model to approximate the rheological behavior of Bingham type materials [26, 20, 2].

We are aware that the no-slip condition in fluid mechanics means that the fluid velocity matches the velocity of the solid boundary. Nearly 200 years ago Navier proposed in his original paper on linearly viscous fluids a general boundary condition that permits the possibility of slip at a solid boundary. This boundary condition assumes that the tangential velocity of the fluid relative to the solid at a point on its surface is proportional to the tangential stress acting at that point. The constant of proportionality between these two quantities may be termed a coefficient of sliding friction (the slip parameter), which is assumed to depend on the nature of the fluid and the solid surface [14]. Some experimental and theoretical studies stated that slip condition could not be ruled out as an important element to understanding of certain characteristic flow [1].

The fluid flows in the presence of magnetic field has promising applications in engineering, chemistry, physics, the polymer industry and metallurgy. Some examples include controlling the rate of cooling, blood plasma, drying, evaporation at the surface of a water body, geothermal reservoirs, thermal insulation, enhanced oil recovery, cooling of nuclear reactors, bleeding reduction during surgeries, hyperthermia etc. Also under the influence of powerful applied magnetic

fields the Hall effects in peristalsis cannot be ignored. In such case the applied magnetic field is powerful or collision frequency is small [16].

There are several studies deal with peristaltic transport with different fluids under the effect of different types of the external forces, as mentioned in [8] and see also, [3, 4, 7, 15]. To the best of our knowledge, no investigation has been made yet to investigate the effect of slip on peristaltic transport for Bingham-Papanastasiou fluid in the presence of Hall current and heat transfer.

In this article the basic equations of motion of the non-Newtonian Bingham-Papanastasiou fluid as well as energy equation are written in section 2. In section 3 the constitutive equations of that fluid are explained. The formulation of the problem investigated mathematically in section 4. In section 5 the stream, velocity and temperature distribution functions; which are calculated analytically and with the help of Mathematica program; are written. Results and discussion is explained in section 6, the conclusion in section 7 and in section 8 the caption of figures are listed. Then the figures which explained the effect of different parameters of the problem on the the heat and velocity are listed, this paper ended with the appendix and list of references.

2 Basic equations

The basic equations which describe the motion of non-Newtonian fluid with heat transfer can be written as

Continuity equation

$$\nabla \cdot \underline{V} = 0, \tag{1}$$

Momentum equation

$$\rho \frac{d\,\underline{V}}{dt} = -\nabla P + \nabla \cdot \underline{S} + \underline{J} \wedge \underline{B} \tag{2}$$

Energy equation

$$\rho c_p \frac{d\,T}{dt} = k_1 \nabla^2 T + \underline{S} \cdot \nabla \underline{V} - \nabla \cdot \underline{q}_r + Q(T - T_0), \tag{3}$$

where

$$\underline{J} = \sigma \left[(\underline{V} \wedge \underline{B}) - \frac{1}{e\, n_e} (\underline{J} \wedge \underline{B}) \right],$$

$\underline{V}$ is fluid velocity vector, ρ is the density of the fluid, P is the pressure, $\underline{S}$ is the extra-stress tensor (S_{ij}), $\underline{J}$ is the current density vector including the Hall effect, σ is the electric conductivity, e is the electric charge, n_e is the number density of electrons, $\underline{B} = (0, 0, B_0)$ is the uniform magnetic field with magnetic flux density, T is temperature, k_1 is the thermal conductivity, $\frac{d}{dt}$ denotes the material time derivative and ∇^2 is the Laplacian operator, Q is heat generation, $\underline{q}_r$ the radiation heat flux vector.

3 The constitutive equations

The regularized constitutive equation proposed by Papanastasiou [21] is

$$\underline{S} = \left[\mu + \frac{S_0(1-\exp(-m\dot{\gamma})}{\dot{\gamma}}\right]\underline{\dot{\gamma}}, \tag{4}$$

where μ is the plastic viscosity, S_0 is the yield stress, m is a stress growth exponent and $\underline{\dot{\gamma}}$ denote the rate of strain tensor;

$$\underline{\dot{\gamma}} = \nabla\underline{V} + (\nabla\underline{V})^{\mathsf{T}} \tag{5}$$

($\nabla\underline{V}$ is the velocity-gradient tensor and $(\nabla\underline{V})^{\mathsf{T}}$ is its transpose) and $\dot{\gamma}$ is the magnitude of the rate of strain tensor,

$$\dot{\gamma} = |\underline{\dot{\gamma}}| = \sqrt{\frac{1}{2}\,II_{\underline{\dot{\gamma}}}} = \sqrt{\frac{1}{2}\,\underline{\dot{\gamma}} : \underline{\dot{\gamma}}} = \sqrt{\frac{1}{2}\sum_i\sum_j \dot{\gamma}_{ij}\dot{\gamma}_{ji}}\,, \tag{6}$$

where $II_{\dot{\gamma}}$ is the second invariant of $\underline{\dot{\gamma}}$.

4 Mathematical formulation

Consider flow of fluid in two-dimensional asymmetric channel, X-axis is taken in motion direction while Y-axis is perpendicular on it and (U, V) are the velocity components in X and Y directions respectively as shown in Fig.(1).

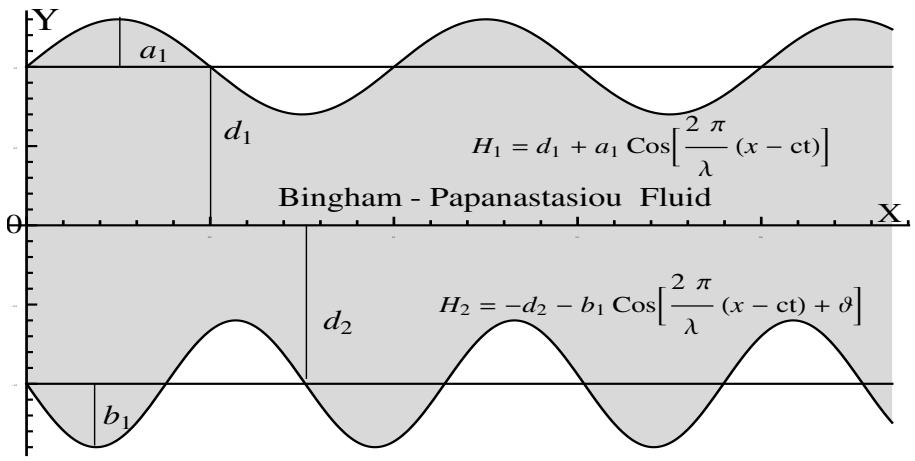

Fig. (1)

The channel asymmetry is produced by choosing the peristaltic wave train on the walls to have different amplitudes and phase, consider the upper and lower channel walls are

$$Y = H_1 = d_1 + a_1 \cos\left[\frac{2\pi}{\lambda}(X - c\,t)\right] \tag{7}$$

$$Y = H_2 = -\,d_2 - \,b_1 \cos\,\left[\frac{2\pi}{\lambda}(X - c\,t) + \vartheta\right] \tag{8}$$

where a_1 and b_1 are the amplitudes of the waves, λ is the wave length, $(d_1 + d_2)$ is the width of the channel and ϑ is the phase difference that varies in the range $0 \leq \vartheta \leq \pi$. Further, a_1, b_1, d_1, d_2 and ϑ satisfy the condition $a_1^2 + b_1^2 + 2a_1 b_1 \cos\vartheta \leq (d_1 + d_2)^2$.

Introducing a wave frame (x, y) moving with the velocity c away from the laboratory frame (X, Y), by the transformations

$$x = X - ct, \quad y = Y, \quad u = U - c, \quad v = V, \quad p\,(x) = P(X, t), \tag{9}$$

where u and v are the fluid velocity components and p is pressure in the wave frame of references.

The equations (1-3) will be on the form

$$\frac{\partial u}{\partial x} + \frac{\partial v}{\partial y} = 0, \tag{10}$$

$$u\frac{\partial u}{\partial x} + v\frac{\partial u}{\partial y} = -\frac{1}{\rho}\,\frac{\partial P}{\partial x} + \frac{\partial S_{xx}}{\partial x} + \frac{\partial S_{xy}}{\partial y} + \frac{\sigma B_0^2}{1 + \mathbf{H}^2}(\mathbf{H}v - (u + c)), \tag{11}$$

$$u\frac{\partial v}{\partial x} + v\frac{\partial v}{\partial y} = -\frac{1}{\rho}\,\frac{\partial P}{\partial y} + \frac{\partial S_{yx}}{\partial x} + \frac{\partial S_{yy}}{\partial y} - \frac{\sigma B_0^2}{1 + \mathbf{H}^2}(v + \mathbf{H}(u + c)), \tag{12}$$

$$\rho c_p \left(u\frac{\partial T}{\partial x} + v\frac{\partial T}{\partial y}\right) = k_1 \left(\frac{\partial^2 T}{\partial x^2} + \frac{\partial^2 T}{\partial y^2}\right) + S_{xx}\frac{\partial u}{\partial x} + S_{xy}\frac{\partial u}{\partial y} + S_{yx}\frac{\partial v}{\partial x} + S_{yy}\frac{\partial v}{\partial y} - \frac{\partial q_r}{\partial y} + Q(T - T_0), \tag{13}$$

where $\mathbf{H} = \frac{\sigma B_0}{e\,n_e}$ is the Hall parameter and the radiative heat flux in the $X-$ direction is considered as negligible compared to $Y-$ direction.

Also, the constitutive equations become

$$S_{xx} = 2\left(\mu + \frac{S_0}{\dot{\gamma}}\left(1 - e^{-m\dot{\gamma}}\right)\right)\frac{\partial u}{\partial x}, \tag{14}$$

$$S_{xy} = S_{yx} = \left(\mu + \frac{S_0}{\dot{\gamma}}\left(1 - e^{-m\dot{\gamma}}\right)\right)\left(\frac{\partial u}{\partial y} + \frac{\partial v}{\partial x}\right), \tag{15}$$

$$S_{yy} = 2\left(\mu + \frac{S_0}{\dot{\gamma}}\left(1 - e^{-m\dot{\gamma}}\right)\right)\frac{\partial v}{\partial y}, \tag{16}$$

with

$$\dot{\gamma} = \left[2\left(\frac{\partial u}{\partial x}\right)^2 + \left(\frac{\partial u}{\partial y} + \frac{\partial v}{\partial x}\right)^2 + 2\left(\frac{\partial v}{\partial y}\right)^2\right]^{\frac{1}{2}}, \tag{17}$$

and the wall equations will be

$$y = d_1 + a_1 \cos \frac{2\pi}{\lambda} x \tag{18}$$

$$y = -\, d_2 - \, b_1 \cos \left[\frac{2\pi}{\lambda} x + \vartheta \right]. \tag{19}$$

Further, by using Rosseland approximation for radiation, the radiative heat flux q_r is given by

$$q_r = -\frac{4}{3} \frac{\sigma_0}{k_0} \frac{\partial T^4}{\partial Y}$$

where σ_0 is Stefan-Boltzman and k_0 is the Rosseland mean absorption coefficient.
Moreover, we suppose that the temperature difference with in the flow is such that T^4 may be expanded in a Taylor series. Hence, expanding T^4 about T_0 and ignoring higher order terms we get:

$$T^4 \cong 4\, T_0^3\, T - 3\, T_0^4$$

i.e

$$q_r = -\frac{16}{3} \frac{\sigma_0 T_0^3}{k_0} \frac{\partial T}{\partial Y} \tag{20}$$

Now introducing the stream function ψ ($u = \frac{\partial \psi}{\partial y} = \psi_y, v = -\frac{\partial \psi}{\partial x} = -\psi_x$) and the following non-dimensional variables

$$\bar{x} = \frac{x}{\lambda}, \quad \bar{y} = \frac{y}{d_1}, \quad \delta = \frac{d_1}{\lambda}, \quad \bar{u} = \frac{u}{c}, \quad \bar{v} = \frac{v}{\delta c}, \quad \bar{t} = \frac{c\, t}{\lambda}, \quad a = \frac{a_1}{d_1},$$

$$b = \frac{b_1}{d_1}, \quad d = \frac{d_2}{d_1}, \quad h_1 = \frac{H_1}{d_1}, \quad h_2 = \frac{H_2}{d_1}, \quad \bar{\psi} = \frac{\psi}{c\; d_1}, \quad \bar{S} = \frac{d}{\mu c} S$$

$$\bar{\dot{\gamma}} = \frac{d_1\; \dot{\gamma}}{c}, \quad \bar{p} = \frac{d_1^2\; p}{\mu\; \lambda\; c}, \quad R = \frac{\rho c\; d_1}{\mu}, \quad \mathcal{K} = \frac{\sigma B_0^2 d_1^2}{\mu}, \quad \Theta = \frac{T - T_0}{T_w - T_0}, \tag{21}$$

after dropping bars and under the assumptions of long wave length ($\delta \ll 1$) and low Reynolds number, the equation of continuity is simply verified.
Equations (11 - 13), using eq. (20), become

$$\frac{\partial S_{xy}}{\partial y} - \frac{\partial p}{\partial x} - \mathcal{H}^2 \left(\frac{\partial \psi}{\partial y} + 1 \right) = 0 \tag{22}$$

$$\frac{\partial p}{\partial y} = 0, \tag{23}$$

$$\left(1 + \frac{4}{3R_n} \right) \frac{\partial^2 \Theta}{\partial y^2} + P_r\; G\; \Theta + P_r\; E_c\; S_{xy} \frac{\partial^2 \psi}{\partial y^2} = 0, \tag{24}$$

Also, equations (14 - 17) become

$$S_{xx} = 0 \tag{25}$$

$$S_{xy} = \left[1 + \frac{B_n}{|\dot{\gamma}|}\left(1 - e^{-M|\dot{\gamma}|}\right)\right]\left(\frac{\partial^2 \psi}{\partial y^2}\right), \tag{26}$$

$$S_{yy} = 0 \tag{27}$$

$$|\dot{\gamma}| = \frac{\partial^2 \psi}{\partial y^2}. \tag{28}$$

So we can write

$$S_{xy} = \left[1 + \frac{B_n}{\psi_{yy}}\left(1 - e^{-M\psi_{yy}}\right)\right]\psi_{yy} \tag{29}$$

and for small values of M we will get

$$S_{xy} = (1 + B_n M)\psi_{yy} \tag{30}$$

where $\mathcal{H}^2 = \frac{\mathcal{K}}{1+\mathbf{H}^2}$, $E_c = \frac{\mu c^2}{k_1 \Delta T} = \frac{c^2}{c_p \Delta T}$ is the Eckert number, $B_n = \frac{d_1}{\mu c} S_0$ is Bingham number, $M = \frac{c\ m}{d_1}$ is the dimensionless stress growth exponent, $P_r = \frac{\mu C_p}{k_1}$ is the Prantdel number, $R_n = \frac{k_1 k_0}{4\sigma_0 T_0^3}$ is the radiation parameter, $G = \frac{Q d_1^2}{\mu C_p}$ is the generation parameter.

By eliminating the pressure between (22),(23) and then using (30) we have

$$(1 + B_n M)\,\psi_{yyyy} - \mathcal{H}^2 \psi_{yy} = 0 \tag{31}$$

also, equation (24) will take the form

$$\left(1 + \frac{4}{3R_n}\right)\frac{\partial^2 \Theta}{\partial y^2} + P_r\ G\ \Theta + P_r\ E_c (1 + B_n M)(\psi_{yy})^2 = 0 \tag{32}$$

It is obvious that when $B_n = 0$ equations (31) and (32) will represent the equations of motion and energy of ordinary Newtonian fluid.

Further more, after applying equation (21) on equations (18) and (19) the upper and lower channel walls in dimensionless forms will be

$$y = h_1 = 1 + a\ \cos 2\pi x, \tag{33}$$

$$y = h_2 = -d - b\ (\cos 2\pi x + \vartheta). \tag{34}$$

Also, the non-dimensional appropriate boundary conditions will be

$$\psi = \frac{q}{2}, \qquad \psi_y + \beta\ \psi_{yy} = -1, \qquad \Theta = 1, \quad at\ y = h_1, \tag{35}$$

$$\psi = -\frac{q}{2}, \qquad \psi_y - \beta\ \psi_{yy} = -1, \qquad \Theta = 0, \quad at\ y = h_2, \tag{36}$$

where q is the flux and β is the non-dimensional slip parameter.

5 Solution of the problem

Through introducing the boundary conditions (35 -36) into (31, 32) the stream function will be

$$\psi = [l_7 (h_1 + h_2 - 2y) + 2 (l_8 \sinh \alpha (y - h_1) + l_9 \cosh \alpha (y - h_1) + h_1 - 2y) \\ +2 (l_{10} \sinh \alpha (y - h_2) + l_{11} \cosh \alpha (y - h_2) - h_2)] l_{12}$$

so the velocity in x-direction will be

$$u = [-2l_7 + 2 (l_8 \alpha \cosh \alpha (y - h_1) + l_9 \alpha \sinh \alpha (y - h_1) - 2) \\ +2 (l_{10} \alpha \cosh \alpha (y - h_2) + l_{11} \alpha \sinh \alpha (y - h_2))] l_{12}$$

and the temperature distribution equation will be

$$\Theta = l_{14}(\alpha^4 K^2 E_c l_{11}^2 \left(3R_n \left(4\alpha^2 - GP_r (\cosh \alpha (-h_1 - h_2 + 2y) - 1)\right) + 16\alpha^2\right)) + A_1 \sinh(\zeta y) + A_2 \cosh(\zeta y)$$

Where $\alpha, \zeta, l_1 - l_{14}, A_1$ andA_2 are given in the Appendix.

6 Results and discussion

In order to have an estimate of the quantitative effects of the various parameters involved in the results of the present analysis we used the softwares MATHEMATICA program. The numerical evaluations of the analytical results are obtained for the velocity u and temperature Θ.

Figures (2-10) illustrated the effect of some parameters of the problem on the temperature Θ. In Fig.(2), we observed that Θ increases with Bingham number B_n. Fig.(3) showed the effect of Eckert number E_c, we noticed that Θ increases with E_c. Fig.(4) illustrated the effect of heat generation parameter G, it is obvious that Θ increases with G.

From Fig.(5) we deduced that Θ increases with increasing of Hall parameter $\mathbf{H}$. In Fig.(6) it is obvious that Θ increases with increasing of the growth parameter M, while Θ decreases with increasing of the phase angle ϑ as shown in Fig.(7) (at $\vartheta = 0$ refers to the case of symmetric channel).

Also Figs.(8) and (9) explained that Θ increases with Prantdel number P_r and radiation parameter R_n. It is clear that Θ decreases with increasing of the slip parameter β as shown in Fig.(10).

Figures (11-15) illustrated the effect of some parameters of the problem on the velocity u.
We observed that u increases with B_n, $\mathbf{H}$, M and ϑ as obtained from Figs.(11-14), while u decreases with the slip parameter β as illustrated in Fig.(15).

7 Conclusion

The problem of two dimensional peristaltic flow of a non-Newtonian Bingham-Papanastasiou fluid with heat transfer, through asymmetric channel, under the influence of slip boundary condition and Hall currents is formed. The equations governing this motion have been solved analytically under the conditions of low Reynolds number and long wave length approximation, subjected to a set of appropriate boundary conditions. The expressions of velocity and temperature distribution have been evaluated for different parameters and have been shown graphically through a set of figures, we have concluded that:

1- the temperature distribution and velocity increase with increasing of Hall parameter **H**.
2- the temperature distribution and velocity decrease with increasing of the slip parameter β.

8 Caption of figures

Fig.(1) The geometry of the problem.

Fig.(2) The temperature distribution Θ is plotted against y for different values of Bingham number B_n when $a = 0.5$, $b = 0.3$, $d = 0.5$, $x = 1$, $\vartheta = \pi$, $q = 0.5$, $\mathcal{K} = 1.2$, $\beta = 0.5$, $\mathbf{H} = 0.1$, $M = 10$, $E_c = 0.1$, $P_r = 0.5$, $R_n = 3$, $G = 1$.

Fig.(3) The temperature distribution Θ is plotted against y for different values of Eckert number E_c when $a = 0.5$, $b = 0.3$, $d = 0.5$, $x = 1$, $\vartheta = \pi$, $q = 0.5$, $\mathcal{K} = 1.2$, $\beta = 0.5$, $\mathbf{H} = 0.1$, $M = 10$, $B_n = 1$, $P_r = 0.5$, $R_n = 3$, $E_c = 0.1$.

Fig.(4) The temperature distribution Θ is plotted against y for different values of heat generation parameter G when $a = 0.5$, $b = 0.3$, $d = 0.5$, $x = 1$, $\vartheta = \pi$, $q = 0.5$, $\mathcal{K} = 1.2$, $\beta = 0.5$, $\mathbf{H} = 0.1$, $M = 10$, $B_n = 1$, $P_r = 0.5$, $R_n = 3$, $G = 1$.

Fig.(5) The temperature distribution Θ is plotted against y for different values of Hall parameter $\mathbf{H}$ when $a = 0.5$, $b = 0.3$, $d = 0.5$, $x = 1$, $\vartheta = \pi$, $q = 0.5$, $\mathcal{K} = 15$, $\beta = 0.5$, $E_c = 0.5$, $M = 10$, $B_n = 1$, $P_r = 0.5$, $R_n = 3$, $G = 1$.

Fig.(6) The temperature distribution Θ is plotted against y for different values of the growth parameter M when $a = 0.5$, $b = 0.3$, $d = 0.5$, $x = 1$, $\vartheta = \pi$, $q = 0.5$, $\mathcal{K} = 1.2$, $\beta = 0.5$, $E_c = 0.5$, $\mathbf{H} = 0.1$, $B_n = 1$, $P_r = 0.5$, $R_n = 3$, $G = 1$.

Fig.(7) The temperature distribution Θ is plotted against y for different values of the phase angle ϑ when $a = 0.5$, $b = 0.3$, $d = 0.5$, $x = 1$, $q = 0.5$, $\mathcal{K} = 1.2$, $\beta = 0.5$, $E_c = 0.1$, $M = 10$, $\mathbf{H} = 0.1$, $B_n = 1$, $P_r = 3$, $R_n = 5$, $G = 0.3$.

Fig.(8) The temperature distribution Θ is plotted against y for different values of the Prantdel number P_r when $a = 0.5$, $b = 0.3$, $d = 0.5$, $x = 1$, $q = 0.5$, $\vartheta = \pi$, $\mathcal{K} = 1.2$, $\beta = 0.5$, $E_c = 0.1$, $M = 10$, $\mathbf{H} = 0.1$, $B_n = 1$, $R_n = 3$, $G = 0.3$.

Fig.(9) The temperature distribution Θ is plotted against y for different values of the radiation parameter R_n when $a = 0.5$, $b = 0.3$, $d = 0.5$, $x = 1$, $q = 0.5$, $\vartheta = \pi$, $\mathcal{K} = 1.2$, $\beta = 0.5$, $E_c = 0.1$, $M = 10$, $\mathbf{H} = 0.1$, $B_n = 1$, $P_r = 3$, $G = 0.3$.

Fig.(10) The temperature distribution Θ is plotted against y for different values of the slip parameter β when $a = 0.5$, $b = 0.3$, $d = 0.5$, $x = 1$, $q = 0.5$, $\mathcal{K} = 1.2$, $R_n = 3$, $E_c = 0.1$, $M = 10$, $\mathbf{H} = 0.1$, $B_n = 1$, $\vartheta = \pi$, $P_r = 0.5$, $G = 1$.

Fig.(11) The velocity u is plotted against y for different values of the Bingham number B_n when $a = 0.5$, $b = 0.3$, $d = 0.5$, $x = 1$, $q = 0.5$, $\vartheta = \pi$, $\beta = 0.2$, $\mathcal{K} = 1.2$, $M = 100$, $\mathbf{H} = 1$.

Fig.(12) The velocity u is plotted against y for different values of the Hall parameter $\mathbf{H}$ when $a = 0.5$, $b = 0.3$, $d = 0.5$, $x = 1$, $q = 0.5$, $\vartheta = \pi$, $\beta = 0.5$, $\mathcal{K} = 1.2$, $M = 100$, $B_n = 1$.

Fig.(13) The velocity u is plotted against y for different values of the growth parameter M when $a = 0.5$, $b = 0.3$, $d = 0.5$, $x = 1$, $q = 0.5$, $\vartheta = \frac{\pi}{2}$, $\beta = 0.5$, $\mathcal{K} = 10$, $\mathbf{H} = 1$, $B_n = 2$.

Fig.(14) The velocity u is plotted against y for different values of the phase angle ϑ when $a = 0.5$, $b = 0.3$, $d = 0.5$, $x = 1$, $q = 0.5$, $M = 10$, $\beta = 0.2$, $\mathcal{K} = 1.2$, $\mathbf{H} = 1$, $B_n = 5$.

Fig.(15) The velocity u is plotted against y for different values of the slip parameter β when $a = 0.5$, $b = 0.3$, $d = 0.5$, $x = 1$, $q = 0.5$, $M = 10$, $\vartheta = \frac{\pi}{2}$, $\mathcal{K} = 1.2$, $\mathbf{H} = 1$, $B_n = 5$.

The list of figures

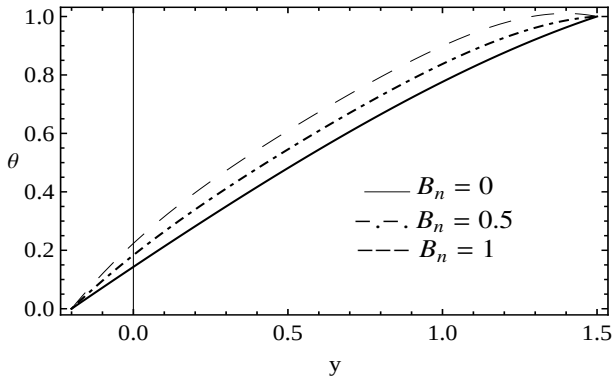

Fig.(2)

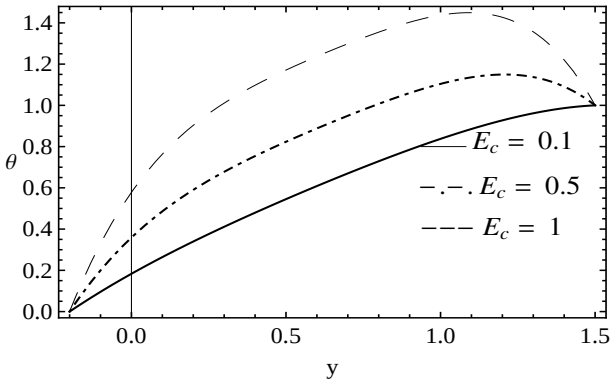

Fig.(3)

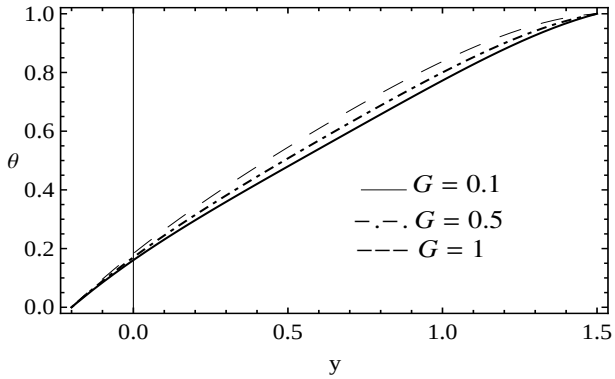

Fig.(4)

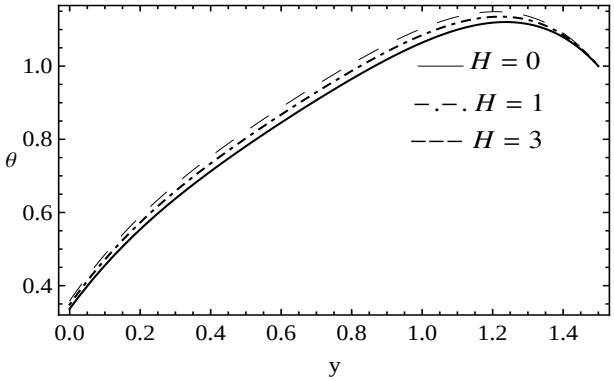

Fig.(5)

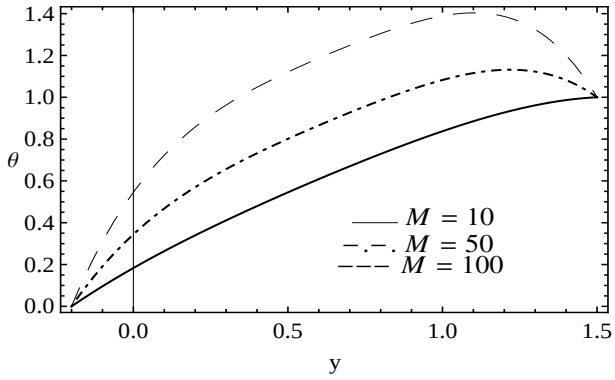

Fig.(6)

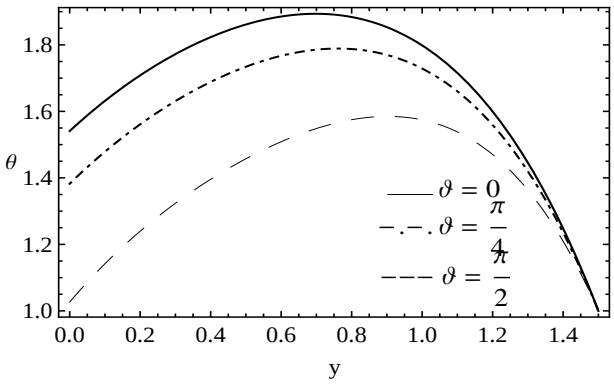

Fig.(7)

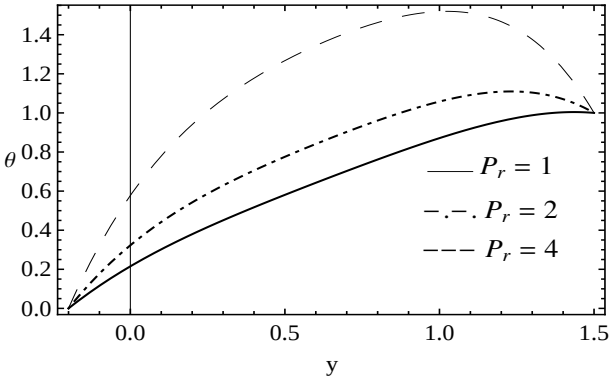

Fig.(8)

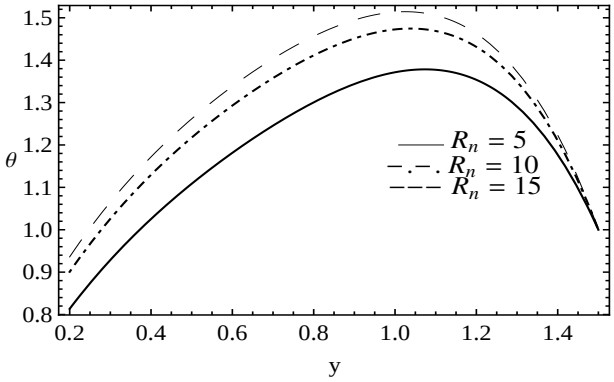

Fig.(9)

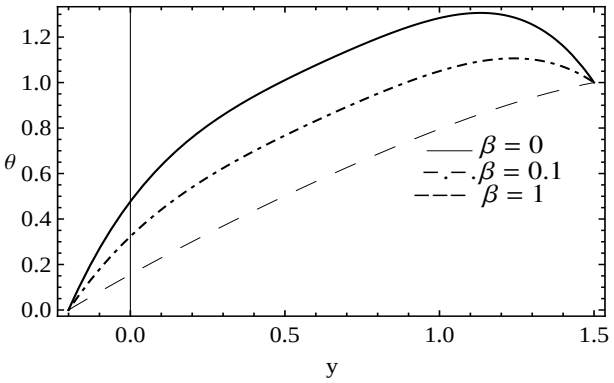

Fig.(10)

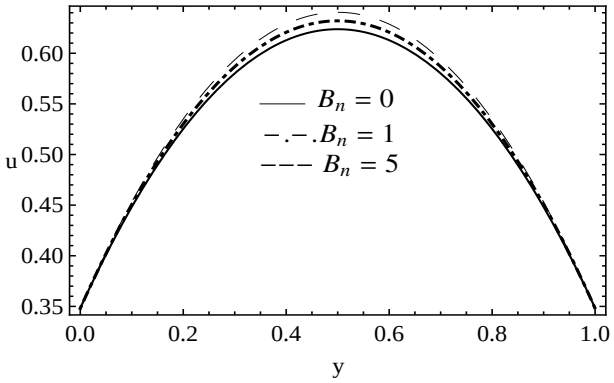

Fig.(11)

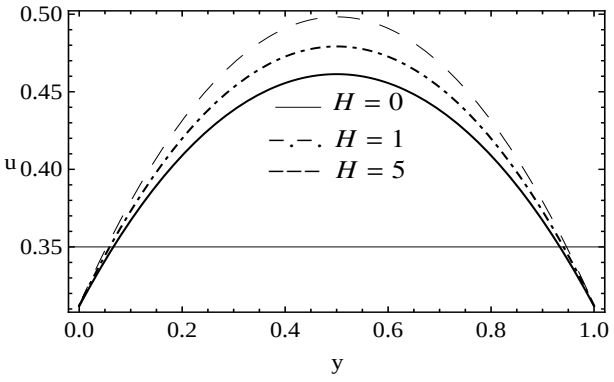

Fig.(12)

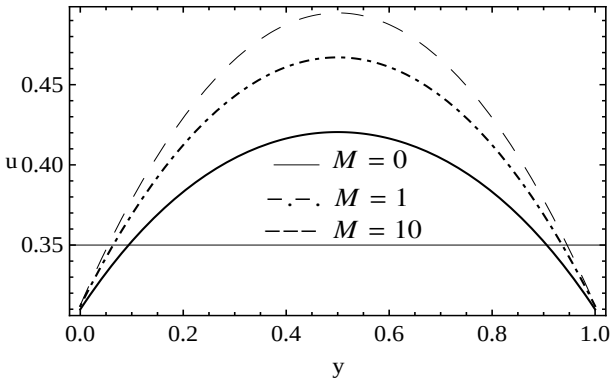

Fig.(13)

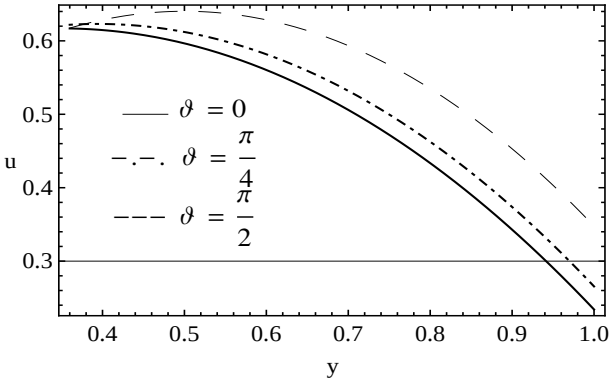

Fig.(14)

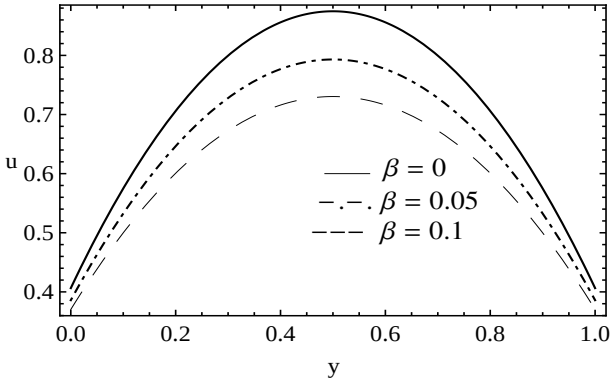

Fig.(15)

The Appendix

$\alpha = \frac{\mathcal{H}}{\sqrt{(1+B_n M)}}$, $\zeta = \sqrt{\frac{3GR_nP_r}{-3R_n-4}}$, $l_1 = \frac{\alpha}{2}(h_1 - h_2)$, $l_2 = 2\alpha\left((h_1 - h_2)\left(\alpha^2\beta^2 + 1\right) - 2\beta\right)$,
$l_3 = 4\left(\alpha^2\beta(h_1 - h_2) - 1\right)$, $l_4 = l_2\sinh 2l_1 + l_3\cosh 2l_1 + 4$, $l_5 = -\alpha\left(q\alpha^2\beta^2 + 2\beta + q\right)$, $l_6 = -2\left(q\alpha^2\beta + 1\right)$,
$l_7 = l_5\sinh 2l_1 + l_6\cosh 2l_1$, $l_8 = -\alpha\beta(h_1 + h_2 + q)$, $l_9 = (h_1 + h_2 + q)$, $l_{10} = \alpha\beta(h_1 - h_2 + q)$,
$l_{11} = (h_1 - h_2 + q)$, $l_{12} = \frac{1}{l_4}$, $l_{14} = \frac{1}{l_{13}}$, $l_{13} = 8G\left((\alpha\beta l_1 - 1)\sinh l_1 + l_1\cosh l_1)\right)^2\left(3R_n(GP_r + 4\alpha^2) + 16\alpha^2\right)$,
$A_1 = l_{14}[\text{cosech}(\zeta(h_1 - h_2))(\alpha^4K^2A_cl_{11}^2(\cosh(h_1\zeta) - \cosh(h_2\zeta))(3R_n(4\alpha^2 - GP_r(\cosh(2l_1) - 1)) + 16\alpha^2) + l_{13}\cosh(h_2\zeta)]$,
$A_2 = -l_{14}[\text{cosech}(\zeta(h_1 - h_2))(\alpha^4K^2A_cl_{11}^2(\sinh(h_1\zeta) + \sinh(h_2\zeta))(3R_n(4\alpha^2 - GP_r(\cosh(-2l_1) - 1)) + 16\alpha^2))$
$+ l_{13}\sinh(h_2\zeta)]$,

References

[1] Abo Elkhair, R.E.S., *Lie point symmetries for amagneto couple stress fluid in a porous channel with expanding or contracting walls and slip boundary condition*, Journal of the Egyptian Mathematical Society, 24, (2016), 656 - 665.

[2] Alexandrou, A.N., Menn, Ph.L., Georgiou, G. and Entov, V., *Flow instabilities of Herschel-Bulkley fluids*, J. Non-Newtonian Fluid Mech., 116, (2003), 19 -32.

[3] Bhattia, M.M. and Rashidi, M.M.,*Study of heat and mass transfer with Joule heating on magnetohydrodynamic (MHD) peristaltic blood flow under the influence of Hall effect*, Propulsion and Power Research, 6(3),2017,177185.

[4] Bhattia, M.M., Ali Abbas, M. and Rashid, M.M., *Combine effects of Magnetohydrodynamics (MHD) and partial slip on peristaltic Blood flow of Ree-Eyring fluid with wall properties*, Engineering Science and Technology, an International Journal, 19, (2016), 1497-1502.

[5] Bingham, E.C., *An investigation of the laws of plastic flow*, Bulletin of the Bureau of Standards, 13, (1916), 309 -353.

[6] Dimakopoulos, Y., Pavlidis, M. and Tsamopoulos, J., *Steady bubble rise in Herschel-Bulkley fluids and comparison of predictions via the Augmented Lagrangian Method with those via the Papanastasiou model*, Journal of Non-Newtonian Fluid Mechanics, 200, (2013), 34 - 51.

[7] Eldabe,N.T., Elogail, M.A., Elshaboury, S.M. and Alfaisal A.H.,*Hall effects on the peristaltic transport of Williamson fluid through a porous medium with heat and mass transfer*, Applied Mathematical Modelling, 40, (2016), 315-328.

[8] Eldabe, N. T. M., Zaghrout, A. S. Shawky, H. M. and Awad, A. S., *Peristaltic transport of micropolar fluid through porous medium in a symmetric channel with heat and mass transfer in the presence of generation and radiation*, African Journal of Mathematics and Computer Science Research, 6(6), (2013), 121-129.

[9] El-Shehawey, E.F., Eldabe, N.T., El-ghzey, E.M. and Ebaid, A., *Peristaltic transport in an asymmetric channel through a porous medium*, Applied Math. and Computation, 182, (2006), 140 -150.

[10] El-Shehawey, E.F. and Husseny, S.Z.A., *Effects of porous boundaries on peristaltic transport through a porous medium*, Acta Mech., 143, (2000), 165 -177.

[11] Eytan, O., Jaffa, A.J. and Elad, D., *Peristaltic flow in a tapered channel: application to ambryo transport within the uterine cavity*, Med. Eng. and Phys., 23, (2001), 473 -482.

[12] Fung, Y.C. and Yih, C.S., *Peristaltic transport*, J. Applied Mechanics, 35, (1968), 669-675.

[13] Fusi, L. and Farina, A., *Flow of a Bingham fluid in a non symmetric inclined channel*, Journal of Non-Newtonian Fluid Mechanics, 238, (2016), 24-32.

[14] Gharsseldien, Z.M., Mekheimer, Kh.S. and Awad, A.S., *The influence of slippage on trapping and reflux limits with peristalsis through an asymmetric channel*, Applied Bionics and Biomechanics, 7(2), 2010, 95 -108.

[15] Hayat,T., Aslam, N., Rafiq, M. and Alsaadi, F.E., *Hall and Joule heating effects on peristaltic flow of Powell-Eyring liquid in an inclined symmetric channel*, Results in Physics,7, (2017), 518528.

[16] Hayat, T., Zahir, H., Tanveer, A. and Alsaedi, A., *Influences of Hall current and chemical reaction in mixed convective peristaltic flow of Prandt lfluid*, Journal of Magnetism and Magnetic Materials, 407, (2016), 321-327.

[17] Kefayati, G.H.R. and Huilgol, R.R., *Lattice Boltzmann Method for simulation of mixed convection of a Bingham fluid in a lid-driven cavity*, International Journal of Heat and Mass Transfer, 103, (2016), 725 -743.

[18] Mekheimer, Kh.S., *Nonlinear peristaltic transport through a porous medium in an inclined planar channel*, J. Porous Media, 6(3), (2003), 189 -201.

[19] Mishra, M. and Rao, A.R., *Peristaltic transport of a Newtonian fluid in an asymmetric channel*, Z. angew. Math. Phys., 54, (2003), 532 - 550.

[20] Mitsoulis, E., *Flows of viscoplastic materials: models and computations*, Rheology Reviews, (2007), 135 -178.

[21] Papanastasiou, T.C., *Flows of materials with yield*, J. Rheol., 31, (1987), 385 - 404.

[22] Soto, H.P. , Martins-Costa, M.L., Fonseca, C. and Frey, S., *A Numerical Investigation of Inertia Flows of Bingham-Papanastasiou Fluids by an Extra Stress-Pressure-Velocity Galerkin Least-Squares Method*, J. of the Braz. Soc. of Mech. Sci. and Eng., 33(5), (2010), 450 -460.

[23] Srivastava, L.M. and Srivastava, V.P., *Peristaltic transport of a two-layered model of physiological fluid*, J. Biomech., 15(4), (1982), 257-265.

[24] Thakur, P., Mittal, Sh., Tiwari, N. and Chhabra, R.P., *The motion of a rotating circula rcylinder in a stream of Bingham plastic fluid*, Journal of Non-Newtonian Fluid Mechanics, 235, (2016), 29 - 46.

[25] Turan, O., Yigit, S. and Chakraborty, N., *Numerical investigation of mixed convection of Bingham fluids in cylindrical enclosures with heated rotating top wall*, International Journal of Heat and Mass Transfer, 108, (2017), 1850 -1869.

[26] Zhu, H., Kim, Y.D. and DeKee, D., *Non-Newtonian fluids with a yield stress*, J. Non-Newtonian Fluid Mech., 129, (2005), 177-181.